Efficient Simulation of Strong System-Environment Interactions

Javier Prior,[1,2] Alex W. Chin,[3] Susana F. Huelga,[3] and Martin B. Plenio[3,2]

[1]*Departamento de Física Aplicada, Universidad Politécnica de Cartagena, Cartagena 30202, Spain*
[2]*QOLS, The Blackett Laboratory, Prince Consort Road, Imperial College, London, SW7 2BW, United Kingdom*
[3]*Institut für Theoretische Physik, Albert-Einstein-Allee 11, Universität Ulm, D-89069 Ulm, Germany*

(Received 14 April 2010; revised manuscript received 1 July 2010; published 30 July 2010)

Multicomponent quantum systems in strong interaction with their environment are receiving increasing attention due to their importance in a variety of contexts, ranging from solid state quantum information processing to the quantum dynamics of biomolecular aggregates. Unfortunately, these systems are difficult to simulate as the system-bath interactions cannot be treated perturbatively and standard approaches are invalid or inefficient. Here we combine the time-dependent density matrix renormalization group with techniques from the theory of orthogonal polynomials to provide an efficient method for simulating open quantum systems, including spin-boson models and their generalizations to multicomponent systems.

DOI: 10.1103/PhysRevLett.105.050404 PACS numbers: 05.30.−d, 03.65.Yz, 03.67.−a, 05.60.Gg

Introduction.—Dissipation and decoherence caused by noisy, fluctuating environments are fundamental and ubiquitous phenomena which appear in all quantum experiments. While initially thought to simply destroy quantum signatures, it was later realized that environmental noise can in fact be instrumental for maintaining quantum correlations in the steady state [1]. Recently, coherence and decoherence have also been shown to play important roles in the excitation energy transport (EET) of some photosynthetic pigment-protein complexes (PPCs) in which long-lasting coherence has been observed [2–4]. As a result, novel emphasis is being placed on better understanding the interplay between coherent and incoherent quantum dynamics arising from environmental interactions [5]. Ultimately, this understanding may facilitate the development of noise-assisted devices and, potentially, light-harvesting systems with increased efficiency.

To date, the dynamics of open quantum systems and, in particular, noise-assisted transport [5] are frequently investigated in terms of simple models in which dephasing and relaxation are treated with Lindblad or Bloch-Redfield master equations. These methods are both based on the assumptions of weak system-bath coupling and the Markov approximation. However, assuming that the correlation time of the environments is much faster than the system dynamics is frequently not justified in many realistic systems. For instance, in typical PPCs the dynamical time scales of the bath can be comparable or even slower than the EET dynamics [6,7]. Moreover, in the limit of slow bath dynamics, perturbative treatments of the system-environment coupling cannot be used even if the system-bath coupling is intrinsically weak [6,8]. Recently, important steps have been taken towards the development of fully nonperturbative simulations of biological EET, such as the numerical hierarchy technique and the numerical path integral [6,9,10]. There are, however, limitations concerning the allowed spectral density of the bath, and these techniques are expected to become less efficient with decreasing temperatures and highly structured environments.

Given the general lack of information about the real protein spectral densities in PPCs, a technique is required that can simulate EET for arbitrary spectral densities and coupling strengths, thus allowing experiments carried out under different conditions, including low temperatures, to be analyzed within one framework. A similar situation is encountered in solid state qubit implementations, where the microscopic details behind the dephasing caused by spurious two-level fluctuators still needs to be fully clarified [11].

Here we address these issues by developing a method that combines an exact analytical mapping of the problem onto an effective 1D system and the time-adaptive density matrix renormalization group (t-DMRG) technique [12]. This approach produces results without any restrictions on the strength of system-bath coupling, and the results have a known and controllable accuracy. Although the richly structured environments used in the PPC literature are taken as examples, it should be emphasized that this new simulation tool is completely general and can be applied to any system linearly coupled to bosonic or fermionic environments of arbitrary spectral density. Importantly, our method also provides complete information about the evolving state of the environment and opens the door to detailed studies of the system-bath correlations which give rise to long-lasting coherences, entanglement, and other novel effects.

The model.—We demonstrate our approach to open-system dynamics by considering an elementary model of a PPC, a dimer molecule consisting of two pigments (henceforth referred to as ''sites''). The dimer's internal dynamics are described by a Hamiltonian $H_S = \frac{\epsilon_1}{2}\sigma_{1z} + \frac{\epsilon_2}{2}\sigma_{2z} + J(\sigma_{1+}\sigma_{2-} + \sigma_{2+}\sigma_{1-})$, where σ_{i+}, σ_{i-}, and σ_{iz} are standard Pauli creation, annihilation, and z matrices,

respectively, for the ith site of the dimer. The spin-down state $\sigma_{iz}|\downarrow_i\rangle = -|\downarrow_i\rangle$ represents the ground state of the site, and the spin-up state represents a single local excitation which can hop between sites with a tunneling amplitude J. Each site i interacts with its own continuous bath of harmonic oscillators described by creation and annihilation operators $a_i^\dagger(k)$ and $a_i(k)$, respectively, which satisfy the continuum commutation relation $[a_i(k), a_j^\dagger(k')] = \delta_{ij}\delta(k-k')$. The site-environment interaction H_I and the environment Hamiltonian H_B can then be written as

$$H_I = \sum_{i=1,2} \frac{(1+\sigma_{iz})}{4} \int_0^1 h(k)[a_i(k) + a_i^\dagger(k)]dk, \quad (1)$$

$$H_B = \sum_{i=1,2} \int_0^1 g(k) a_i^\dagger(k) a_i(k) dk. \quad (2)$$

We assume here that both baths have identical dispersions $g(k)$ and coupling strengths $h(k)$, although this is not a requirement of the method. The spectrum of bath frequencies is limited by a high-frequency cutoff ω_c. The effects of the site-bath interactions are completely determined by specifying the spectral function $J(\omega)$ of the bath [13]. By introducing the inverse function for the dispersion $g^{-1}(k)$, $J(\omega)$ is defined for the continuous oscillators by $J(\omega) = \pi h^2[g^{-1}(\omega)]\frac{dg^{-1}(\omega)}{d\omega}$ [14].

In order to simulate the dynamics of $H = H_S + H_I + H_B$ with t-DMRG, we first need to transform H into an effective 1D representation [9,14,15]. In the numerical renormalization group (NRG) approach to open quantum systems, the transformation is usually implemented via an approximate discretization of the bath degrees of freedom and then a recursive numerical procedure [15]. Here, we transform H exactly by representing the bath with a new set of bosonic operators given by $b_{in} = \int_0^1 U_n(k) a_i(k) dk$ and $b_{in}^\dagger = \int_0^1 U_n(k) a_i^\dagger(k) dk$, where $n = 0, 1, 2, \ldots, \infty$. We now choose $U_n(k) = h(k)\rho_n^{-1}\pi_n(k)$, where ρ_n is a normalization constant and $\pi_n(k)$ is the nth monic polynomial of a sequence of orthogonal polynomials (OPs) defined by the inner product $\int_0^1 h^2(k)\pi_n(k)\pi_m(k)dk = \rho_n^2\delta_{nm}$. By using the properties of OPs, the transformation can be seen to be manifestly orthogonal, and the new modes obey bosonic commutation relation $[b_n, b_m^\dagger] = \delta_{nm}$ [16]. The spectral function $J(\omega)$ does not uniquely specify both $g(k)$ and $h(k)$; however, the choice $g(k) = \omega_c k$ fixes $h^2(k) = \pi^{-1}\omega_c J[g(k)]$.

Expressing H in terms of the new modes generates a Hamiltonian of the form shown in Fig. 1 and is described by $\tilde{H} = H_S + H_{\rm IC} + H_C$, where the system-chain interaction $H_{\rm IC}$ and chain Hamiltonian H_C are given by

$$H_{\rm IC} = \sum_{i=1,2} \sqrt{\frac{\eta}{\pi}} \frac{(1+\sigma_{iz})}{4} (b_{i0} + b_{i0}^\dagger), \quad (3)$$

$$H_C = \sum_{i=1,2} \sum_{n=0}^{\infty} \epsilon_{in} b_{in}^\dagger b_{in} + (t_{in} b_{in+1}^\dagger b_{in} + \text{H.c.}). \quad (4)$$

The new modes of the chain have frequencies ϵ_{jn} and nearest-neighbor couplings t_{jn} $(j = 1, 2)$. The coupling of site j to the first member of its chain is given by $\eta = \int_0^{\omega_c} J(\omega)d\omega$. The nearest-neighbor chain structure is a direct consequence of using the basis of OPs and a linear dispersion $g(k)$. When the new operators are substituted into Eq. (1), the effective coupling strength of the nth mode of the chain to the site is $\propto \int_0^1 h^2(k)\pi_n(k)dk$, which is only nonzero for $n = 0$ due to the orthogonality of the $\pi_n(x)$ and the fact that $\pi_0(x) = 1$. Similarly, when the new modes are substituted into Eq. (2), modes n and m couple to each other with a strength $\propto \int_0^1 h^2(k)k\pi_n(k)\pi_m(k)dk = \int_0^1 h^2(k)[\alpha_n\pi_n(k) + \beta_n\pi_{n-1}(k) + \pi_{n+1}(k)]\pi_m(k)dk$, where we have used the standard three-term recurrence relation obeyed by monic OPs to replace the product $k\pi_n(k)$. After this step, orthogonality guarantees nearest-neighbor couplings only, and the whole system of sites and oscillators can be arranged in an infinite 1D chain as shown in Fig. 1(b). Note also that the specific form of the system operator in Eq. (1) is of no importance for the transformation, and the mapping will also apply, for example, for environments that induce or suppress spontaneous decay of excitations such as those found in photonic crystals [17].

This exact mapping and its mathematical properties, which also hold for fermionic baths, can be found in Ref. [16], where analytical formulas for ϵ_n and t_n are given for several important classes of continuous and logarithmically discretized baths. When analytical results are not available, we take advantage of the fact that ϵ_{in} and t_{in} are simply related to the recurrence coefficients α_n and β_n introduced above and can be determined accurately by using very stable numerical algorithms for OPs [16,18]. This is important as the NRG recursive technique quickly develops numerical instabilities [14], and sharp spectral features like those we will later consider make this method

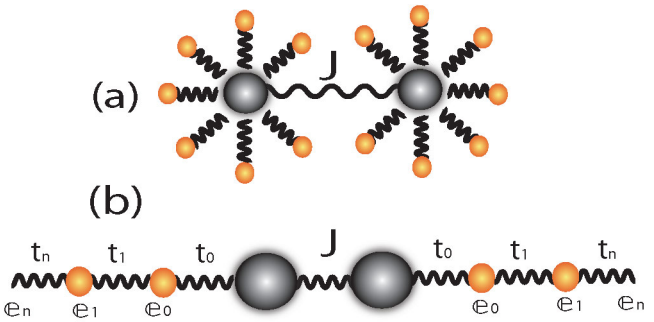

FIG. 1 (color online). (a) The standard Hamiltonian has each site of the dimer interacting with its surrounding bath in a starlike configuration. (b) After a unitary transformation of the bosonic modes only, an infinite harmonic 1D chain Hamiltonian is generated with frequencies ϵ_n and nearest-neighbor couplings t_n.

even more unstable. The analytical mapping also generates a number of interesting physical insights. Mathematical analysis of these transformations demonstrates that, for *any* spectral density which is strictly bigger than zero in its domain, $\epsilon_{in} \to \omega_c/2$, $t_{in} \to \omega_c/4$ as $n \to \infty$. This is the mathematical expression of the fact that we expect that excitations are eventually lost to the environment irreversibly. A translationally invariant harmonic chain with this ratio of ϵ_n to t_n has a gapless dispersion with bandwidth ω_c, and excitations can escape down the chain without being scattered back towards the system. Thus the buildup of excitations in any region of the chain is limited, and hence correlations are expected to be bounded. This in turn suggests that DMRG will converge quickly [19]. The universal asymptotics of environments revealed by this analysis are discussed in Ref. [16].

The overdamped Brownian oscillator spectral density.—We now demonstrate the implementation of our method with some specific spectral densities of relevance for PPCs in photosynthetic organisms. To start with, we look at the overdamped Brownian oscillator (OBO) spectral density which has previously been studied in the high temperature limit [6]. The bath in our simulations is at $T = 0$ K, although finite temperatures can be simulated by using standard extensions of DMRG to mixed states [20]. The OBO spectral density is described by $J(\omega) = \frac{8\lambda\gamma\omega}{\omega^2+\gamma^2}$, where the reorganization energy λ is defined by $\lambda = \frac{1}{4\pi} \times \int_0^{\omega_c} J(\omega)\omega^{-1} d\omega$ and is taken as our measure of the system-bath coupling strength. The parameter γ sets the dynamical response time of the bath [6,7]. The initial condition is the separable state of zero excitations in the bath and one excitation on site one. This initial condition is used throughout this work, although our approach allows us to simulate any initially correlated state. In all the t-DMRG simulations in this Letter, we found that the results converged to less than 0.1% with just 11 bosonic levels per site, 30 Schmidt coefficients, and 100 chain sites over the whole dynamics [12].

Figure 2 shows the population on site 1 as a function of time for various values of λ. For $\lambda \leq 100$ cm^{-1} we find damped oscillations which persist for at least 1 ps. For larger λ, coherent dynamics are always seen for a few hundred femtoseconds before the dynamics becomes incoherent, although as λ increases the duration of coherent motion becomes shorter. For $\lambda \geq 200$ cm^{-1} the incoherent relaxation rate decreases dramatically, and an increasingly large population is trapped on site 1 over the time scale of the simulations. This quantum-Zeno-like phenomenon may be related to the well-studied localization transition found in Ohmic and sub-Ohmic spin-boson models at $T = 0$ K [13]. This is a nonperturbative feature of the dynamics, and similar dynamics have also recently been observed in other studies of the sub-Ohmic spin-boson model [9,21].

Other spectral densities.—We now demonstrate the versatility of our method with respect to the microscopic

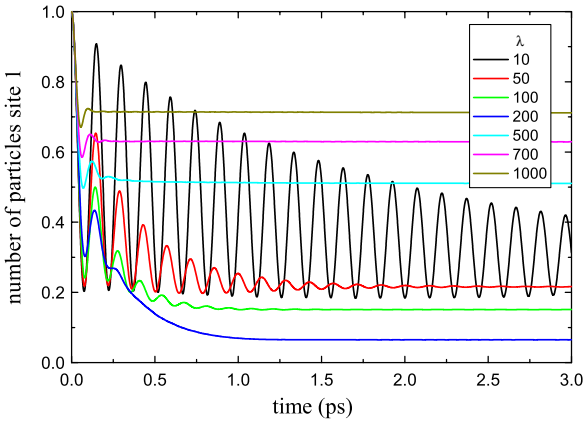

FIG. 2 (color online). Evolutions of the population on site 1 for the overdamped Brownian oscillator at $T = 0$ K and various reorganization energies λ. Simulation parameters are $J = 100$ cm^{-1}, $\epsilon_1 - \epsilon_2 = 100$ cm^{-1}, and $\gamma = 53$ cm^{-1}.

system-bath interactions by considering a much more complex and structured environmental spectral function taken from a recent study of photosynthetic EET. Reference [22] uses a combination of super-Ohmic densities and a coupling to a single effective high-energy mode to model the environment. In our notation this spectral function can be written as

$$J(\omega) = \frac{2\pi\lambda[1000\omega^5 e^{-(\omega/\omega_1)(1/2)} + 4.3\omega^5 e^{-(\omega/\omega_2)(1/2)}]}{9!(1000\omega_1^5 + 4.3\omega_2^5)} + 4\pi S_H \omega_H^2 \delta(\omega - \omega_H), \quad (5)$$

where we have kept the relative contributions of the two continuous parts of the spectral density as they are in Ref. [22] but have also introduced an overall reorganization energy λ to be used as a free parameter. The coupling to the high-energy mode is fixed, and the parameters of the simulation are $J = 100$ cm^{-1}, $\epsilon_1 - \epsilon_2 = 100$ cm^{-1}, $\omega_1 = 0.5$ cm^{-1}, $\omega_2 = 1.95$ cm^{-1}, $\omega_H = 180$ cm^{-1}, $\omega_c = 1000$ cm^{-1}, and $S_H = 0.22$ [22]. With these values the continuous part of $J(\omega)$ extends over a frequency range of about 900 cm^{-1}, and ω_H is almost resonant with the energy difference (224 cm^{-1}) of the dimer eigenstates of H_s as the coupling strength of this mode to a site is 84 cm^{-1}.

The chain transformation and DMRG method offers numerical advantages for spectral functions which contain delta functions or damped resonances, as discrete modes of the environment do not have to be considered part of the system Hamiltonian and are simply represented by modified chain parameters. This allows an arbitrary number of undamped or dissipative modes to be included without any increase in the complexity of the simulation. Other approaches which treat discrete modes on an equal footing as the system always grow in complexity with the number of modes [23]. The interaction with the near-resonant oscillator has a pronounced effect on the population dynamics, and Fig. 3 shows how this coupling leads to a coherent

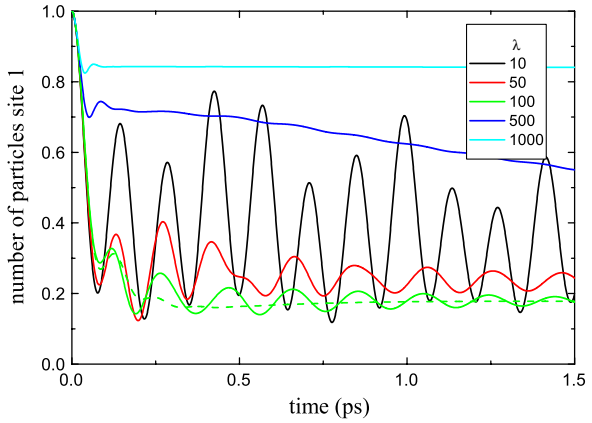

FIG. 3 (color online). Evolutions of the population on site 1 for the spectral function of Eq. (5) at various reorganization energies λ and $T = 0$ K. Dimer parameters are $J = 100\ \mathrm{cm}^{-1}$ and $\epsilon_1 - \epsilon_2 = 100\ \mathrm{cm}^{-1}$. The dashed line shows how the dynamics when the high-energy mode is decoupled.

beating effect which periodically suppresses population oscillations for $\lambda \leq 300\ \mathrm{cm}^{-1}$. In situations where site 2 might transfer population to another system, such a coherent suppression of oscillations could lead to an enhancement of EET from the dimer to that system. As λ increases, the continuous part of the spectral density dominates the dynamics, and we observe qualitatively similar behavior to the dynamics obtained in Fig. 2. We note that the trapping dynamics for large λ is less severe for this super-Ohmic $J(\omega)$ [24], although the dynamics are still highly non-Markovian for strong coupling.

A particularly striking feature of Fig. 3 is that, in the regime of optimal EET ($\lambda \sim 100\ \mathrm{cm}^{-1}$), the high-energy mode leads to low amplitude oscillations which persist for at least 1.5 ps. When the high-energy mode is decoupled, coherent oscillations vanish for $\lambda = 100\ \mathrm{cm}^{-1}$ after just 0.3 ps. Experimental observation of such persistent undamped oscillations after a fast population transfer could thus indicate the presence of discrete high-energy modes in the environment of PPCs [5].

Conclusions.—Combining an analytical chain transformation with t-DMRG methods, we have introduced an efficient and highly accurate method for the simulation of archetypal models of open quantum systems. We now plan to explore the important question of the role and persistence of coherence in biological EET, by using existing DMRG techniques to consider finite temperatures, multiple sites, and spatially correlated baths. We also expect the method to be relevant for a variety of problems in condensed matter and quantum information.

This work is supported by the EU projects CORNER and QAP and the Humboldt Foundation. J. P. was supported by the Fundacion Seneca, Grants No. 11602/EE2/09 and No. 11920/PI/09-J, and Ministerio de Ciencia e Innovacion Project No. FIS2009-13483-C02-02. We thank F. Caruso for his assistance with this work.

[1] M. B. Plenio and S. F. Huelga, Phys. Rev. Lett. **88**, 197901 (2002); L. Hartmann, W. Dür, and H.-J. Briegel, Phys. Rev. A **74**, 052304 (2006).
[2] M. Mohseni *et al.*, J. Chem. Phys. **129**, 174106 (2008).
[3] M. B. Plenio and S. F. Huelga, New J. Phys. **10**, 113019 (2008).
[4] G. S. Engel *et al.*, Nature (London) **446**, 782 (2007); G. Panitchayangkoon *et al.*, Proc. Natl. Acad. Sci. U.S.A. **107**, 12766 (2010); T. R. Calhoun *et al.*, J. Phys. Chem. B **113**, 16 291 (2009); E. Collini *et al.*, Nature (London) **463**, 644 (2010).
[5] F. Caruso *et al.*, J. Chem. Phys. **131**, 105106 (2009); A. W. Chin *et al.*, New J. Phys. **12**, 065002 (2010); P. Rebentrost *et al.*, New J. Phys. **11**, 033003 (2009).
[6] A. Ishizaki and G. R. Fleming, J. Chem. Phys. **130**, 234111 (2009); Proc. Natl. Acad. Sci. U.S.A. **106**, 17 255 (2009).
[7] M. Thorwart *et al.*, Chem. Phys. Lett. **478**, 234 (2009).
[8] P. Nalbach and M. Thorwart, arXiv:0911.5590.
[9] F. B. Anders, R. Bulla, and M. Vojta, Phys. Rev. Lett. **98**, 210402 (2007).
[10] A. Ishizaki and Y. Tanimura, J. Phys. Soc. Jpn. **74**, 3131 (2005).
[11] J. Schriefl *et al.*, New J. Phys. **8**, 1 (2006); L. Faoro and L. B. Ioffe, Phys. Rev. Lett. **100**, 227005 (2008).
[12] S. R. White, Phys. Rev. Lett. **69**, 2863 (1992); U. Schollwoeck, Rev. Mod. Phys. **77**, 259 (2005); G. Vidal, Phys. Rev. Lett. **93**, 040502 (2004); A. Daley *et al.*, J. Stat. Mech. (2004) P04005; S. R. White and A. E. Feiguin, Phys. Rev. Lett. **93**, 076401 (2004).
[13] A. J. Leggett *et al.*, Rev. Mod. Phys. **59**, 1 (1987).
[14] R. Bulla *et al.*, Phys. Rev. B **71** 045122 (2005); R. Bulla, T. A. Costi, and T. Pruschke, Rev. Mod. Phys. **80**, 395 (2008).
[15] Guo *et al.*, Phys. Rev. B **79**, 115137 (2009).
[16] A. W. Chin *et al.*, arXiv:1006.4507.
[17] D. G. Angelakis, P. L. Knight, and E. Paspalakis, Contemp. Phys. **45**, 303 (2004).
[18] W. Gautschi, ACM Trans. Math. Softw. **20**, 21 (1994).
[19] J. Eisert, M. Cramer, and M. B. Plenio, Rev. Mod. Phys. **82**, 277 (2010).
[20] R. Rosenbach *et al.* (to be published).
[21] P. Nalbach and M. Thorwart, Phys. Rev. B **81**, 054308 (2010).
[22] J. Adolphs and T. Renger, Biophys. J. **91**, 2778 (2006).
[23] H. Tamura, J. Chem. Phys. **130**, 214705 (2009).
[24] S. Jang *et al.*, J. Chem. Phys. **129**, 101104 (2008).